

Mechanical Properties and Network Structure of Phenol Resin Crosslinked Hydrogenated Acrylonitrile-Butadiene Rubber

Noboru Osaka, Masahiro Kato, Hiromu Saito

Department of Organic and Polymer Materials Chemistry, Tokyo University of Agriculture and Technology, Koganei, Tokyo 184-8588, Japan

Correspondence to: H. Saito (E-mail: hsaitou@cc.tuat.ac.jp)

ABSTRACT: The tough and stretchable crosslinked hydrogenated acrylonitrile-butadiene rubber (HNBR) could be prepared by resol type phenol resin as a crosslinker. The mechanical properties and the network structure of the phenol resin crosslinked HNBR were investigated by comparing with those of the peroxide crosslinked HNBR having the higher crosslink density and the heterogeneous network structure. The elastic modulus and the strain at break of the phenol resin crosslinked HNBR were much higher than those of the peroxide one. The residual strain was below 20 % after stretching up to 650 % and then releasing from the cramps. Since the crosslink density is low, the high elastic modulus and the good recovery deformation are attributed to the stiffness and rigidity of the crosslink junctions obtained by phenol resin. Small-angle X-ray scattering measurements revealed that the network structure is spatially homogeneous and the results of the wide angle X-ray diffraction indicate that the strain-induced crystallization is suppressed, which enable the longer elongation. © 2013 Wiley Periodicals, Inc. *J. Appl. Polym. Sci.* 129: 3396–3403, 2013

KEYWORDS: crosslinking; mechanical properties; rubber; structure-property relations; X-ray

Received 21 November 2012; accepted 10 January 2013; published online 27 February 2013

DOI: 10.1002/app.39010

INTRODUCTION

Crosslinking is crucial for good elastic properties of rubbers. By crosslinking the rubber, the stable and three-dimensional network structure is formed. The network structure can be changed by using different crosslinking agents.^{1–8} The mechanical properties of the crosslinked rubbers depend on the network structure; i.e., the elastic modulus and the recovery deformation behavior are improved due to the enhanced entropic elasticity by network structure.^{9–14}

Network structure of crosslinked rubber is characterized by several parameters: (1) crosslink density, (2) rigidity of crosslink junctions, and (3) presence of heterogeneity in the network. The classical and later the more sophisticated rubber theories, such as the affine^{15,16} or the phantom network models^{17,18} and the tube model,^{19–21} describe the rubber elasticity on the basis of the densities of crosslinks and entanglements. However, actual network structures are far from the ideal state and their mechanical properties are difficult to explain only by the densities of crosslinks and entanglements. For example, peroxide crosslinked rubber exhibits high modulus due to the short and rigid C—C crosslink junctions, while sulfur crosslinked rubber exhibits more elongation and hence the higher stress at break due to the flexible and labile C—S—C crosslink junctions.^{5,22,23}

However, the peroxide crosslinked rubber has disadvantages such as low tensile strength and low flex resistance due to the presence of the heterogeneous network structure with densely crosslinked region and loosely crosslinked one.²⁴ Owing to the heterogeneous network structure, the applied stress during the deformation is locally concentrated, which readily leads to the break.^{25,26}

Phenolic resin is a well-known thermosetting resin²⁷ and the crosslinked network by phenolic resin is highly rigid due to the bulky nature of benzene rings. The phenolic resin is also used as the crosslinking agent on the diene elastomer such as natural rubber,²⁸ ethylene propylene diene monomer rubber,^{29,30} and acrylonitrile-butadiene rubber (NBR).^{31,32} Phenolic resin forms the chroman and methylene bridges with the carbon double bond and the allylic hydrogen, respectively. While the C—C bonding energy is comparable to that of the peroxide crosslinking,²⁹ the stiffness, and rigidity of phenolic molecule improve the mechanical properties of the rubber.^{33,34} However, the effect of the network structure on the mechanical properties has not been elucidated.

In this study, we investigated the mechanical properties of hydrogenated acrylonitrile-butadiene rubber (HNBR) crosslinked by various amounts of phenol resin. Here HNBR was

used as the rubber specimen because its low content of the carbon double bond and its compatibility with phenol resin are expected to prevent to form heterogeneity in the network. The characteristic mechanical properties were revealed by comparing with those of the peroxide crosslinked HNBR, and were discussed in terms of the network structure: (1) crosslink density and (2) rigidity of crosslink points by the results of swelling, tensile-testing and wide angle X-ray diffraction (WAXD) measurements, and (3) heterogeneity in the network by the result of small angle X-ray scattering (SAXS) measurement.

EXPERIMENTAL

Materials

The hydrogenated acrylonitrile-butadiene rubber (HNBR) used in this study was Zetpol2010 kindly supplied by Nihon Zeon Corp. The weight average molecular weight is 298,000 g/mol and the number averaged molecular weight is 79,200 g/mol. The weight fraction of the acrylonitrile is 36 wt % and the hydrogenation ratio of the butadiene is 96%. Resol type phenol resin (PL-2211, Gun Ei Chemical Industry, Japan) and DCP (Percumyl D-40, NOF Corporation, Japan) were used as crosslinking agents.

HNBR was compounded with ZnO (Yoneyama Yakuhin Kogyo; Japan) and stearic acid (Yoneyama Yakuhin Kogyo; Japan) for the accelerator of crosslinking reaction, and for crosslinking agents (phenol resin or DCP). SnCl₂·H₂O was added as the Lewis acid activator for the crosslinking reaction of phenol resin. The amount of the ingredient compounds is listed in Table I. HNBR and all the compounds were dissolved into chloroform and then the solvent was evaporated under a reduced atmosphere of 10⁻² mmHg at room temperature. To obtain the crosslinked HNBR film with a thickness of 300 μm for the following experiments, the cast film was collected and was melt pressed at 180°C for 20 min. The representative chemical structures of the HNBR crosslinked by DCP and phenol resin are shown in Scheme 1.

Tensile Tests

For the tensile-testing measurement, the film specimen was cut into a rectangle of 30 mm length and 10 mm width. The stress-strain curve of the film specimen was obtained by using a tensile-testing machine (VES05D, Toyoseiki) at a crosshead rate of 20 mm/min at room temperature. For the tensile cycle test, the specimen was stretched up to 650% strain and then released to shrink back at the rate of 20 mm/min.

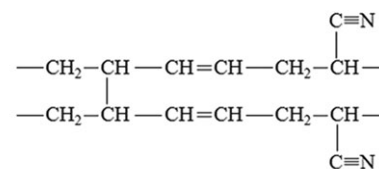
Estimation of Crosslink Density

The crosslink density was estimated from the swelling experiment. The specimen was immersed in dimethyl formamide (DMF) and the volume change by swelling was measured. The

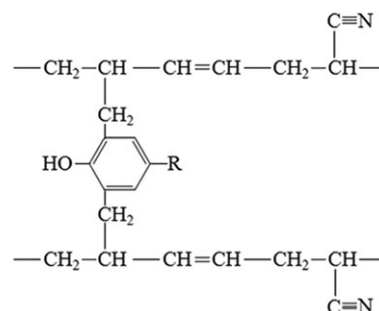
Table I. Recipes of Crosslinked HNBR

	phr
HNBR (Zetpol 2010)	100
DCP or phenol resin	3, 5, 10
ZnO	3
Stearic acid	2
SnCl ₂ ·2H ₂ O	2

DCP cross-linked HNBR



Phenol cross-linked HNBR



Scheme 1. Representative chemical structures of the crosslinked HNBR.

number density of the crosslink ν was estimated from the equilibrium swelling by using the Flory-Rehner equation, which is given by^{23,31}

$$\nu = -1/V_s \left[\frac{\ln(1 - V_r) + V_r + \chi V_r^2}{V_r^{1/3} - V_r/2} \right] \quad (1)$$

where χ is the interaction parameter between polymer and solvent, V_s is the molar volume of solvent and V_r is the volume fraction of the rubber in the swollen crosslinked rubber. χ was calculated to be 0.40 by³⁵

$$\chi = 0.35 + \frac{V_s}{RT} (\delta_p - \delta_s) \quad (2)$$

where V_s is the molar volume of the HNBR segment, δ_p and δ_s are the solubility parameters of HNBR and chloroform of 17.90 and 18.76 MPa^{1/2}, respectively.³⁶ The swelling measurement was carried out several times for each specimen. The obtained densities were averaged and the error ratio of the obtained density was within 5%.

The number density of the crosslink was also estimated from the stress-strain properties in the dry state by using the equation of the classical theory of rubber elasticity, which is given by¹⁰

$$\sigma = \nu kT(\alpha - \alpha^{-2}) \quad (3)$$

where σ is the stress, k is the Boltzmann constant, T is the absolute temperature, and α is the stretching ratio.

Wide-Angle X-ray Diffraction and Small-Angle X-ray Scattering Measurements

WAXD and SAXS measurements were performed by using NANO-Viewer system (Rigaku; Japan). A Cu-K α radiation (46

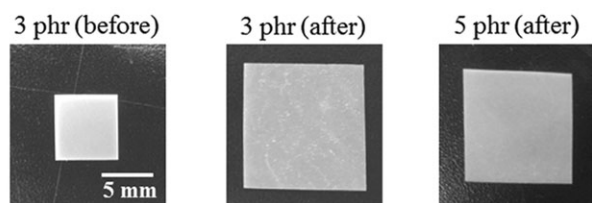
kV, 60 mA) was generated and collimated by a confocal max-flux mirror system. The wavelength was 0.154 nm. The sample to detector distances were 15 mm for WAXD and 700 mm for SAXS, respectively. An imaging plate (IP) (Fujifilm BAS-SR 127) was used as a two-dimensional detector and the IP reading device (R-AXIS Ds3, Rigaku) was used to transform the obtained image into the text data. The exposure times were 15 min for WAXD measurement and 2 h for SAXS measurement, respectively. The scattering intensities were corrected with respect to the exposure time, the sample thickness and the transmittance.

RESULTS AND DISCUSSION

The formation of crosslinked network and the crosslinking state in the crosslinked HNBR was evaluated by swelling experiments. Figure 1 shows photographs of the DCP and phenol resin cross-linked HNBRs with various amounts of crosslinkers immersed in DMF. The DCP crosslinked HNBRs were not dissolved but only swollen in DMF [Figure 1(a)], indicating that the HNBR was crosslinked by DCP above the amount of 3 phr. On the other hand, the HNBR crosslinked with the phenol resin of 5 phr was only swollen in DMF while that with the phenol resin of 3 phr was dissolved in DMF [Figure 1(b)], suggesting that the phenol resin of 5 phr was sufficient to completely crosslink the HNBR while HNBR was only partially crosslinked by the phenol resin of 3 phr. Thus, the crosslinked HNBR could be prepared by using the phenol resin above the amount of 5 phr.

Figure 2 shows the stress–strain properties of the DCP and phenol resin crosslinked HNBRs with various amounts of crosslinkers. The change of the properties with the amount of the crosslinker was small in the DCP crosslinked HNBR [Figure 2(a)]. Stress of the DCP crosslinked HNBR (3 or 5 phr DCP) steeply increased with strain at low strain below 100%, and gradually increased up to the strain at around 600%, then

(a) DCP cross-linked HNBR



(b) phenol resin cross-linked HNBR

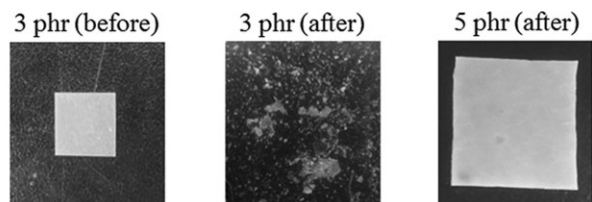


Figure 1. Photographs of the crosslinked HNBR before immersion in DMF and after 24 h from the immersion: (a) DCP crosslinked HNBR, (b) phenol resin crosslinked HNBR.

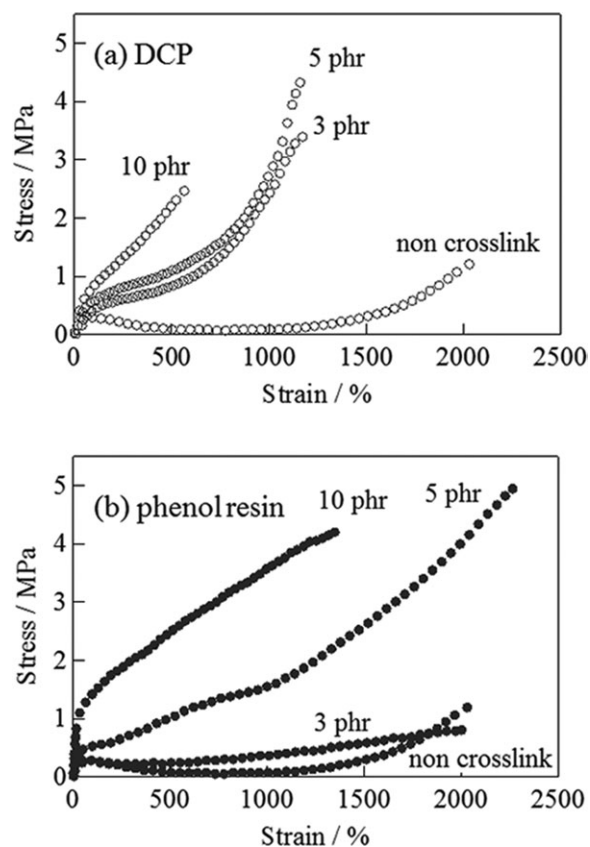


Figure 2. Stress–strain curves of the crosslinked HNBR at various amounts of the crosslinkers: (a) DCP crosslinked HNBR, (b) phenol resin crosslinked HNBR.

increased steeply by stress hardening up to the breaking point at around 1200%. The tensile strength slightly increased as the amount of DCP increased. However, as the amount of DCP increased to 10 phr, the strain and the stress at break decreased in halves. The large reduction of the stress–strain properties at high amount of DCP is attributed to the stress concentration at the small strain due to the significant heterogeneous network structure,²³ as demonstrated later by the SAXS results. On the other hand, the properties of the phenol resin crosslinked HNBR improved successively with increasing the amount of crosslinker. The properties of the phenol resin crosslinked HNBR (3 phr phenol resin) were almost the same to those of the noncrosslinked HNBR because the HNBR was only partially crosslinked by phenol resin as revealed by dissolution in DMF shown in Figure 1(b). However, as the amount of phenol resin increased to above 5 phr, drastic increase in the tensile strength was observed; e.g., the tensile strength at the strain of 500 % increased successively with increasing the amount of phenol resin. The steep increase by stress hardening was observed at the phenol resin of 5 phr and it occurred at much larger strain than that at the same additive amount of DCP. While the stress hardening occurred at the larger strain of 1000%, the stress at break increased to large one about 5 MPa which is comparable with that for the same additive amount of DCP. As the amount of phenol resin increased to 10 phr, the reduction of the strain

and stress at break was small, while the reduction was large in the DCP crosslinked HNBR.

Figure 3 shows the elastic modulus and the strain at break of the DCP and phenol resin crosslinked HNBRs with the amounts of crosslinker, obtained from the stress-strain properties in Figure 2. The elastic modulus and the strain at break of the phenol resin crosslinked HNBR are much higher than those of the DCP crosslinked HNBR at all the amounts of crosslinkers; i.e., the properties of the phenol resin crosslinked HNBR are more than twice as compared with those of the DCP one. These results clearly suggest the successful preparation of the tough and stretchable HNBR rubber crosslinked by phenol resin.

To understand the excellent mechanical properties of the phenol resin crosslinked HNBR, the number density of the crosslinks was estimated by equation 1 from the equilibrium swelling shown in Figure 1 and also by eq. (3) from the initial increase of the stress at low strain shown in Figure 2. Figure 4 shows the number density of the crosslink in the DCP and phenol resin crosslinked HNBRs with the amounts of crosslinker. The number density of the crosslink in the phenol resin crosslinked HNBR estimated by the swelling experiments was smaller than that in the DCP one. As demonstrated in Figure 1, the phenol resin of 3 phr was insufficient to complete the crosslinking while the DCP of 3 phr was sufficient to complete the crosslinking. These results suggest that the crosslinking reaction of the phenol resin is lower than the DCP. On the contrary, the number density of the crosslink in the phenol resin crosslinked HNBR estimated by the tensile-testing measurements were

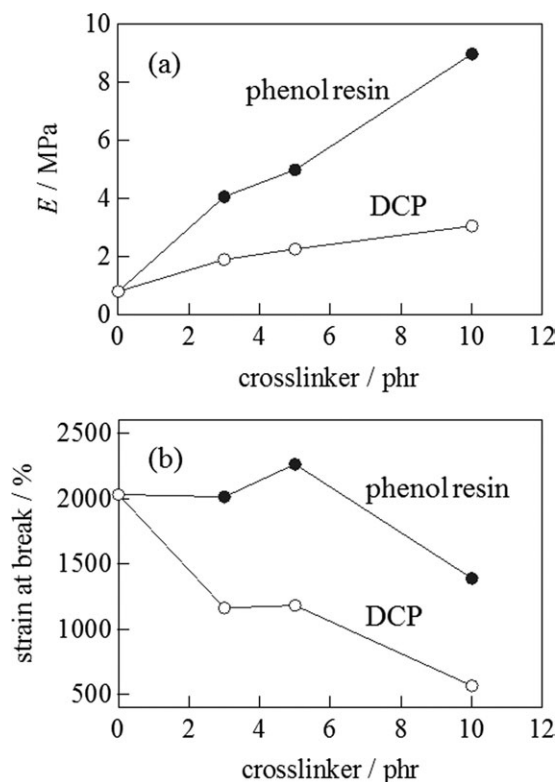


Figure 3. (a) Elastic modulus and (b) strains at break of the DCP and phenol resin crosslinked HNBR.

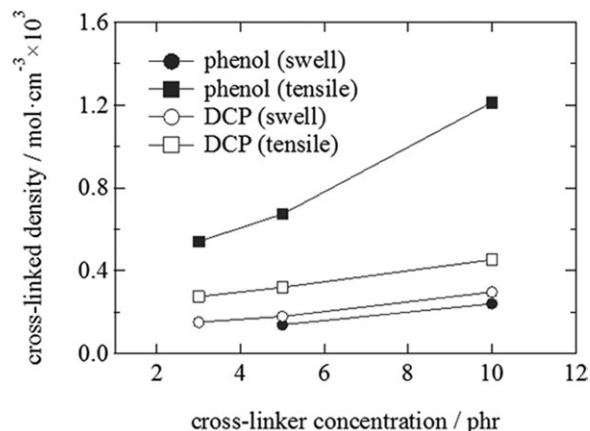


Figure 4. Number density of the crosslinks in the HNBR with the amount of crosslinker estimated by the swelling measurements and the tensile-testing measurements.

much larger than that in the DCP one. Since the number density of the crosslink estimated by the tensile-testing measurements is related to the elastic modulus, the large modulus of the phenol resin crosslinked HNBR shown in Figure 3 is not ascribed to the high crosslink density (number density) but to the stiffness and rigidity of the crosslink junctions obtained by phenol resin as a crosslinking agent. Hence, the bulky nature of the phenol resin highly improves the mechanical strength of the crosslinked HNBR regardless of the low crosslink density (number density) by low crosslinking reaction, which is also exhibited even for the partially crosslinked HNBR (3 phr phenol resin).

The deformation recovery behaviors of the crosslinked HNBRs evaluated by the uniaxial cyclic tensile tests are shown in Figure 5. The deformation hysteresis of the phenol resin crosslinked HNBR is larger than that of the DCP one. The residual strain after the shrink back of the phenol resin crosslinked HNBR is larger than that of the DCP one; e.g., the residual strain of HNBR crosslinked with phenol resin of 5 phr was 125% and that with DCP of 5 phr was 75%. The larger hysteresis and residual strain of the phenol resin crosslinked HNBR might be ascribed to the low crosslink density (number density).

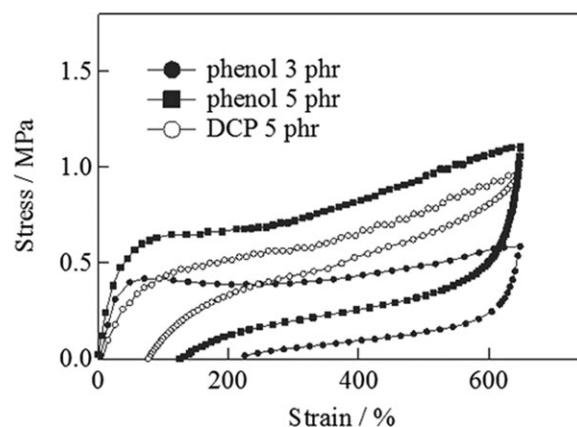


Figure 5. The recovery deformation behaviors of the DCP and phenol resin crosslinked HNBR after elongation to 650% strain.

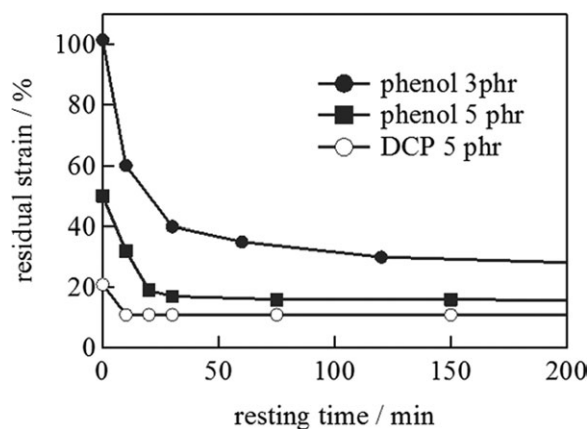


Figure 6. The residual strain of the DCP and phenol resin crosslinked HNBR after release from the clamps as a function of resting time.

Though the crosslinked HNBR showed the large deformation hysteresis and the large residual strain by the uniaxial cyclic tensile tests, the specimen shrank back further by releasing the specimen from the clamps after the shrink back of the cyclic tensile tests. As shown in Figure 6, the phenol resin crosslinked HNBR with phenol resin of 5 phr shrank back to the strain below 20% after releasing for 30 min, which is almost equivalent to the DCP crosslinked HNBR. Thus, the phenol resin crosslinked HNBR with phenol resin above the amount of 5 phr showed the good rubber elasticity for recovery deformation. The good recovery deformation

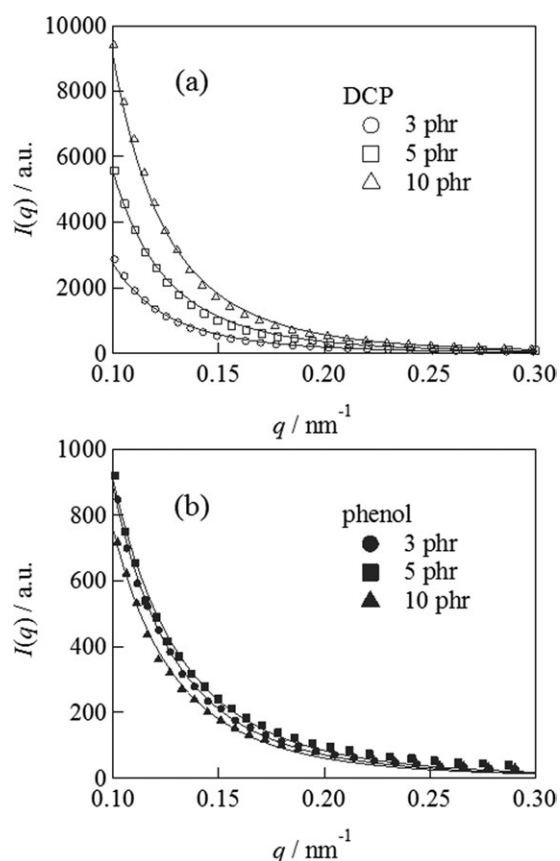


Figure 7. SAXS profiles of the DCP and phenol resin crosslinked HNBR.

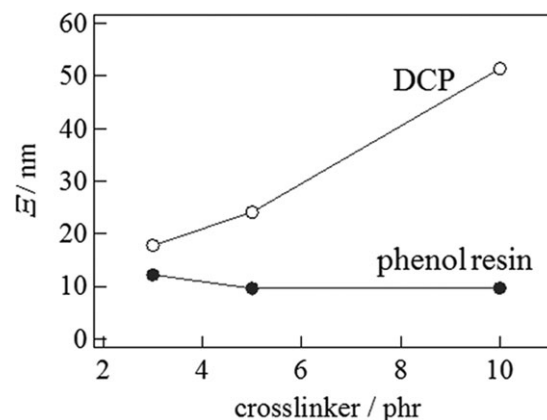


Figure 8. The characteristic sizes of the inhomogeneous structure in the DCP and phenol-resin crosslinked HNBR at various amounts of the crosslinker.

might be attributed to the stiffness and rigidity of the crosslink junctions regardless of the low crosslink density (number density).

SAXS measurements were carried out to clarify the difference in the network structure of the DCP and phenol resin crosslinked HNBRs. The scattering profiles of the crosslinked HNBR with various amounts of crosslinker are shown in Figure 7. Here $I(q)$ is the scattering intensity at q in which q is the scattering vector defined as $q = 4\pi/\lambda \sin(\theta/2)$, λ and θ being the wavelength and the scattering angle, respectively. The DCP crosslinked HNBR showed the strong upturn in the low q region and the intensity increased as the amount of DCP increased [Figure 7(a)]. This strong upturn in the crosslinked rubber originates from the spatially heterogeneous network structure induced during the crosslinking reaction.^{6,8,37,38} Therefore, a large spatial heterogeneity exists in the DCP crosslinked HNBR and it increases as the amount of DCP increases. On the other hand, the scattering intensity of the phenol resin crosslinked HNBR was much lower than that of the DCP one, and the scattering profiles showed no characteristic dependence of the amount of phenol resin [Figure 7(b)].

The scattering profiles were then analyzed by fits using the Debye-Bueche equation^{6,8}:

$$I(q) = \frac{I(0)}{(1 + q^2\Xi^2)^2} \quad (4)$$

where Ξ is the characteristic size of the heterogeneous network structure originating from the density difference between the densely crosslinked region and the loosely crosslinked one.* In Figure 8 is shown the Ξ as a function of the amount of the crosslinker. Ξ of the DCP crosslinked HNBR increased as the amount of DCP increased. On the other hand, the size of Ξ in

*The abbreviations used are: MALDI-TOF, matrix-assisted laser desorption ionization-time-of-flight; ESI-Q-TOF, electrospray ionization-quadrupole-time-of-flight; DDPSC, Donald Danforth Plant Science Center; MALDI, matrix-assisted laser desorption ionization; ESI, electrospray ionization; TOF, time-of-flight; GFP, green fluorescent protein; RNAi, RNA interference; SDS-PAGE, SDS-polyacrylamide gel electrophoresis; OASS, O-acetylserine sulfhydrylase; 2,4-D, 2,4-dichlorophenoxyacetic acid; 2DE, two-dimensional gel electrophoresis; 2D, two-dimensional; YFP, yellow fluorescent protein.

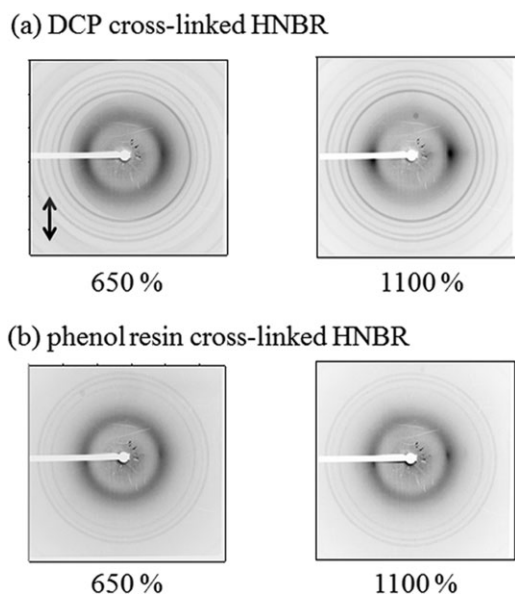


Figure 9. The two-dimensional WAXD patterns of the DCP and phenol resin crosslinked HNBR at various strains.

the phenol resin crosslinked HNBR was much smaller than the DCP one. Also the Ξ of the phenol resin crosslinked HNBR was almost constant with the amount of the phenol resin. These results suggest that the phenol resin crosslinked HNBR is more homogeneous than the DCP one.

In the crosslinking reaction of the peroxide on NBR, the generated radical attaches to a double bond and forms a new crosslink. Then, the radical initiates the reaction between the adjacent double bonds and it forms the densely crosslinked region to yield heterogeneity in the crosslink network, which is further enhanced with increasing the amount of the crosslinker.^{26,39} On the other hand, the phenolic resin would only form the methylene bridge by addition reaction of double bond or substitution reaction of allylic hydrogen and/or the chroman bridged structure on the allylic hydrogen.^{31,32} Although the reaction mechanism is still on debate, our SAXS results suggest that, in the HNBR, the crosslinking reaction with the phenol resin largely depresses the growth of the heterogeneity while the radical reaction by DCP forms the large heterogeneous network structure. As mentioned in the reference 23, spatial heterogeneity in the network causes the stress concentration during the deformation and it induces the break. Thus, the large reduction of the strain and stress at break at high amount of crosslinker in the DCP crosslinked HNBR shown in Figure 2 is attributed to the heterogeneity in the network. On the other hand, owing to the more homogeneous network structure in the phenol resin crosslinked HNBR, the reduction of the strain and stress at break at high amount of crosslinker is suppressed.[†]

[†]Phenol resin crosslinked HNBR should have crosslinks with higher chain length comparing to DCP crosslinked HNBR. The high chain length per crosslinks would make the crosslinks flexible and dangling. This may also suppress the reduction of the strain and stress at break at high amount of crosslinker in the phenol resin crosslinked HNBR.

WAXD measurements were carried out to reveal the difference of the deformation processes between the DCP and phenol resin crosslinked HNBRs from the viewpoint of the strain-induced crystallization of HNBR. Figure 9 shows the two-dimensional WAXD patterns for the HNBR crosslinked by DCP and phenol resin of 5 phr. At 650% strain, which is close to the onset strain of the stress hardening of the DCP crosslinked HNBR, the (020) reflection strongly appeared on the equatorial line in the DCP crosslinked HNBR compared to that in the phenol resin one. This result suggests that the stress hardening observed on the stress-strain curves shown in Figure 2 is attributed to the crystallization of the crosslinked HNBR. At the higher strain of 1100%, the reflection became stronger and sharper, suggesting the enhanced crystallization and orientation of the HNBR. The diffraction intensity at the (020) reflection in the phenol resin crosslinked HNBR is lower than that in the DCP one.

To reveal the orientation behavior of the HNBR, the orientation of crystal component was investigated in detail with the use of the Hermans orientation parameter, f , obtained by azimuthal scanning of the equatorial (020) reflection with the following equations,⁴⁰

$$\langle \cos^2 \theta \rangle = \frac{\int_0^{\pi/2} I_c(\theta) \cos^2 \theta \sin \theta d\theta}{\int_0^{\pi/2} I_c(\theta) \sin \theta d\theta} \quad (5)$$

$$f = \frac{3\langle \cos^2 \theta \rangle - 1}{2} \quad (6)$$

where θ is the azimuthal angle from the stretching direction and $I_c(\theta)$ is the diffraction intensity of crystal component at θ . $I_c(\theta)$ was obtained by subtracting the minimum scattering intensity in the azimuthal scattering profile as the scattering intensity of the amorphous component from the original WAXD intensity.⁴¹ Figure 10 shows the Hermans orientation parameter, f , of the crystal component of crosslinked HNBR at various strains. The absolute value of f in the phenol resin crosslinked HNBR is much lower than that in the DCP one at all the strains, indicating that the orientation of the phenol resin crosslinked HNBR along the stretching direction is much depressed.

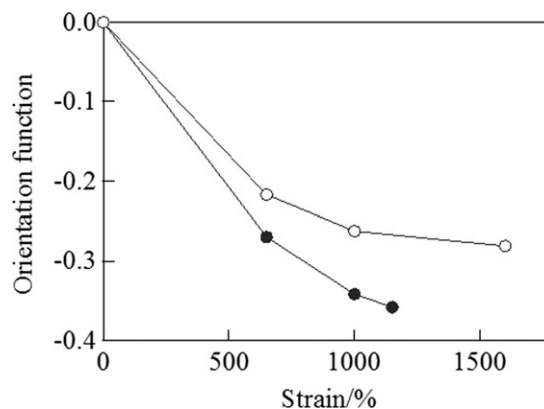
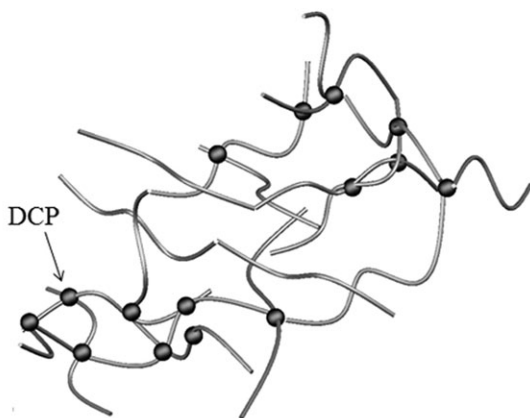


Figure 10. The Hermans orientation parameters of crystal components of the DCP and phenol resin crosslinked HNBR at various strains.

(a) the DCP cross-linked HNBR



(b) the phenol resin cross-linked HNBR

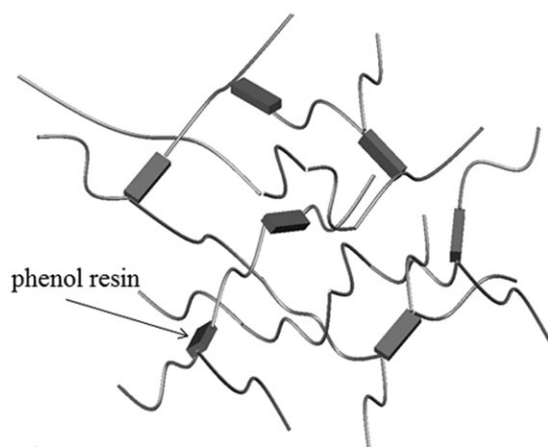


Figure 11. Schematic structures of the DCP and phenol resin HNBR.

The depression of the orientation is attributed to the low crosslink density (number density) and the spatially homogeneous network structure. Owing to the depression of the orientation, the strain-induced crystallization is suppressed and the steep increase of the stress by the stress hardening is delayed in the phenol resin crosslinked HNBR as shown in Figure 2.

The schematics of the structures of the DCP and phenol resin crosslinked HNBRs are shown in Figure 11. In the DCP cross-linked HNBR, the spatially heterogeneous network structure is formed [Figure 11(a)]. During the deformation, the applied stress is enhanced at the locally concentrated region, readily leading to the break. On the other hand, in the phenol resin crosslinked HNBR, more homogeneous network structure with lower crosslink density (number density) is formed by the stiff and rigid phenol resin [Figure 11(b)].

CONCLUSIONS

The tough and stretchable HNBR could be prepared by cross-linking with resol type phenol resin above the amount of 5 phr. The elastic modulus of the phenol resin crosslinked HNBR was larger than that of the DCP one while the crosslink density of

the crosslinked phenol resin was lower. The residual strain after releasing was below 20%, which is almost equivalent to that of the DCP one. They are because the bulky nature of the cross-linked phenol resin gave the stiffness and the rigidity to the network structure. The phenol resin crosslinked HNBR could be elongated to a 2000% strain, which is about twice long of the DCP one. SAXS measurements revealed that the network structure is spatially homogeneous. Therefore, in addition to the low crosslink density, the homogeneity in the network depresses the stress concentration during the uniaxial stretching and the strain-induced crystallization, which enable the longer elongation.

ACKNOWLEDGMENTS

This work was partially supported by the Japan Society for the Promotion of Science (Grant-in-Aid for Young Scientists (B), No. 24750214; Grant-in-Aid for Scientific Research (C), No. 24550246).

REFERENCES

- Ferry, J. D.; Mancke, R. G.; Maekawa, E.; Oyanagi, Y.; Dickie, R. A. *J. Phys. Chem* **1964**, *68*, 3414.
- Maekawa, E.; Mancke, R. G.; Ferry, J. D. *J. Phys. Chem.* **1965**, *69*, 2811.
- Chakraborty, S. K.; Bhowmick, A. K.; De, S. K. *J. Macromol. Sci.; Polym. Rev.* **1981**, *21*, 313.
- Toki, S.; Sics, I.; Ran, S.; Liu, L.; Hsiao, B. S. *Polymer* **2003**, *44*, 6003.
- Rahiman, K. H.; Unnikrishnan, G.; Sujith, A.; Radhakrishnan, C. K. *Mater. Lett.* **2005**, *59*, 633.
- Ikeda, Y.; Higashitani, N.; Hijikata, K.; Kokubo, Y.; Morita, Y.; Shibayama, M.; Osaka, N.; Suzuki, T.; Endo, H.; Kohjiya, S. *Macromolecules* **2009**, *42*, 2741.
- Mani, S.; Cassagnau, P.; Bousmina, M.; Chaumont, P. *Macromolecules* **2009**, *42*, 8460.
- Suzuki, T.; Osaka, N.; Endo, H.; Shibayama, M.; Ikeda, Y.; Asai, H.; Higashitani, N.; Kokubo, Y.; Kohjiya, S. *Macromolecules* **2010**, *43*, 1556.
- Flory, P. J.; Rabjohn, N.; Shaffer, M. C. *J. Polym. Sci. Part B: Polym. Phys.* **1949**, *4*, 225.
- Treloar, L. R. G. *The Physics of Rubber Elasticity*, 3rd ed.; Oxford University Press: New York, **2005**.
- Dossin, L. M.; Graessley, W. W. *Macromolecules* **1979**, *12*, 123.
- Mott, P. H.; Roland, C. M. *Macromolecules* **1996**, *29*, 6941.
- Litvinov, V. M.; Orza, R. A.; Klüppel, M.; Duin, M. V.; Magusin, P. C. M. M. *Macromolecules* **2011**, *44*, 4887.
- Maiti, A.; Weisgraber, T. H.; Gee, R. H.; Small, W.; Alviso, C. T.; Chinn, S. C.; Maxwell, R. S. *Phys. Rev. E* **2011**, *83*, 062801.
- Kuhn, W.; Grün, F.; *Kolloid Z. Z. Polymer* **1943**, *101*, 248.
- Gestoso, P.; Brisson, J. *J. Polym. Sci. Part B: Polym. Phys.* **2002**, *40*, 1601.
- James, H. M.; Guth, E. *J. Chem. Phys.* **1943**, *11*, 455.

18. James, H. M.; Guth, E. J. *Chem. Phys.* **1947**, *15*, 669.
19. Doi, M.; Edwards, S. F. *J. Chem. Soc. Faraday Trans. 2* **1978**, *74*, 1789.
20. Edwards, S. F.; Vilgis, T. A. *Rep. Prog. Phys.* **1988**, *51*, 243.
21. Rubinstein, M.; Panyukov, S. *Macromolecules* **1997**, *30*, 8036.
22. George, S. C.; Knörger, M.; Thomas, S. J. *Membr. Sci.* **1999**, *163*, 1.
23. El-Nemr, K. F. *Mater. Des.* **2011**, *32*, 3361.
24. Valentín, J. L.; Posadas, P.; Fernández-Torres, A.; Malmierca, M. A.; González, L.; Chass, W.; Saalwächter, K. *Macromolecules* **2010**, *43*, 4210.
25. Grobler, J. H. A.; McGill, W. J. *J. Polym. Sci. Part B: Polym. Phys.* **1994**, *32*, 287.
26. González, L.; Rodríguez, A.; Marcos-Fernández, A.; Valentín, J. L.; Fernández-Torres, A. *J. Appl. Polym. Sci.* **2007**, *103*, 3377.
27. Gardziella, A.; Pilato, L. A.; Knop, A. *Phenolic Resins: Chemistry, Applications, Standardization, Safety and Ecology*, 2nd completely rev.; Springer: Berlin, **1999**.
28. Giller, A. *Kautsch. Gummi Kunstst.* **1964**, *17*, 3.
29. Duin, M. V. *Rubber Chem. Technol.* **1995**, *68*, 717.
30. Duin, M. V. *Rubber Chem. Technol.* **2000**, *73*, 706.
31. Achary, P. S.; Ramaswamy, R. *J. Appl. Polym. Sci.* **1998**, *69*, 1187.
32. Liu, L.; Jia, D.; Luo, Y.; Guo, B. *J. Appl. Polym. Sci.* **2006**, *100*, 1905.
33. Wu, C.; Wei, C.; Guo, W.; Wu, C. *J. Appl. Polym. Sci.* **2008**, *109*, 2065.
34. Derakhshandeh, B.; Shojaei, A.; Faghihi, M. *J. Appl. Polym. Sci.* **2008**, *108*, 3808.
35. Rodríguez, F. *Principles of Polymer Systems*, 2nd ed.; McGraw-Hill: New York, **1982**.
36. Choudhury, A.; Bhowmick, A. K.; Ong, C. *Polymer* **2009**, *50*, 201.
37. Norisuye, T.; Masui, N.; Kida, Y.; Ikuta, D.; Kokufuta, E.; Ito, S.; Panyukov, S.; Shibayama, M. *Polymer* **2002**, *43*, 5289.
38. Shibayama, M. *Polym. J.* **2011**, *43*, 18.
39. Valentín, J. L.; Rodríguez, A.; Marcos-Fernández, A.; González, L. *J. Appl. Polym. Sci.* **2005**, *96*, 1.
40. Roe, R.-Y. *Methods of X-Ray and Neutron Scattering in Polymer Science*; Oxford University Press: New York, **2000**.
41. Ran, S.; Zong, X.; Fang, D.; Hsiao, B. S.; Chu, B.; Phillips, R. A. *Macromolecules* **2001**, *34*, 2569.